Supporting Information

Role of cerium oxide in bioactive glasses during catalytic dissociation of hydrogen peroxide

F. Benedetti[1,2], L. Amidani[3], J. S. Pelli Cresi[1,2], F. Boscherini[4,5], S. Valeri[1,2], S. D'Addato[1,2], V. Nicolini[6], G. Malavasi[6], P. Luches[2*]

[1] Dipartimento di Scienze Fisiche Informatiche e Matematiche, Università degli Studi di Modena e Reggio Emilia, Via G. Campi 213/a, 41125 Modena, Italy

[2] Consiglio Nazionale delle Ricerche, Istituto Nanoscienze, Via G. Campi 213/a, 41125 Modena, Italy

[3] European Synchrotron Radiation Facility, BP 220, 38043 Grenoble, France

[4] Department of Physics and Astronomy, University of Bologna, Viale C. Berti Pichat 6/2, 40127 Bologna, Italy

[5] Istituto Officina dei Materiali, Consiglio Nazionale delle Ricerche, Operative Group in Grenoble, c/o ESRF, BP 220, 38043 Grenoble, France

[6] Dipartimento di Scienze Chimiche e Geologiche, Università degli Studi di Modena e Reggio Emilia, Via G. Campi 183, 41125 Modena, Italy

* corresponding author e-mail: paola.luches@nano.cnr.it

Specific surface area

The specific surface area (SSA) of the glasses were evaluated by adsorption of N_2 at a temperature of 77 K using a Micromeritics ASAP 2020 porosimeter.

The samples were outgassed in vacuum at room temperature for 12 hours before the measurements.

The BET model [1] was used to determine the surface area.

The results of the SSA measurements for the samples are summarized in table ST1

Table ST1: Specific Surface Area of the investigated glass samples

SAMPLE	SSA (m^2/g)
H	1.5
K	1
MBG	311
MBG^{4+}	340

Determination of point of zero charge

The PZC (point of zero charge) value was determined for all the investigated samples using two methods:

a) <u>Simplified mass potentiometic titration method [2, 3]</u>
Two identical solutions (blank and sample) were prepared with 3.0 mL of 0.1 M KNO_3 and 6.0 mL of deionized water, and their pH values were measured with a Conductronic 120 pH meter. 1.0 mL of 0.01 M KOH were added to the blank solution and the pH was measured again. 50 mg of the EC precipitate was then added to the sample solution, followed by 1.0 mL of 0.01 M KOH. Both the blank and the sample were then titrated with 0.01 M HNO_3 and the results were plotted. The PZC of each sample was estimated at the point where both titration curves crossed.

b) <u>Salt addition method [4]</u>
This method consists in a simple titration that requires a smaller amount of solid sample than other methods. Here, 0.200g of each EC precipitate was added to 40.0mL of 0.1 M $NaNO_3$ in ten 50-mL plastic beakers. The pH was adjusted using a ThermoElectron Orion 4 Star pH meter to 2, 3, 4, 5, 6, 7, 8, 9, 10 and 11 ($\pm$ 0.1 pH units) with 0.1 M HNO_3 and 0.1 M NaOH as needed in each beaker. These were then shaken for 24 h in a revolving water bath to reach equilibrium (Gyratory water bath shaker

G76). After this time each resulting pH was measured and the initial pH (pH_0) vs. the difference between the initial and final pH values (pH) was plotted. The PZC was taken as the point where pH= 0.
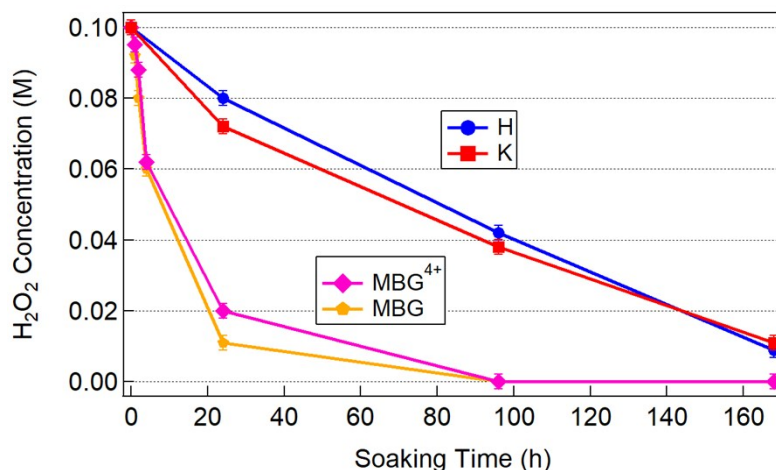

Figure S1: The degradation of H_2O_2 was determined by soaking the glasses in a 0.1 M water solution (glass mass/solution volume = 5 mg/mL) in a stirrer and by determining the residual H_2O_2 concentration by titration with $KMnO_4$. The figure reports the residual H_2O_2 concentration after 1, 2, and 4 h and 1, 4, and 7 days by the H (blue), K (red), MBG (orange) and MBG^{4+} glasses (pink). The decrease is much faster for mesoporous glasses (MBG and MBG^{4+}) than for glasses obtained by melting (H and K). The H and K samples have a comparable dissociation rate, although the K sample contains a lower molar concentration of cerium oxide (3.6 %) compared to the H sample (5.6 %). The data on H glass are reproduced from reference [5].
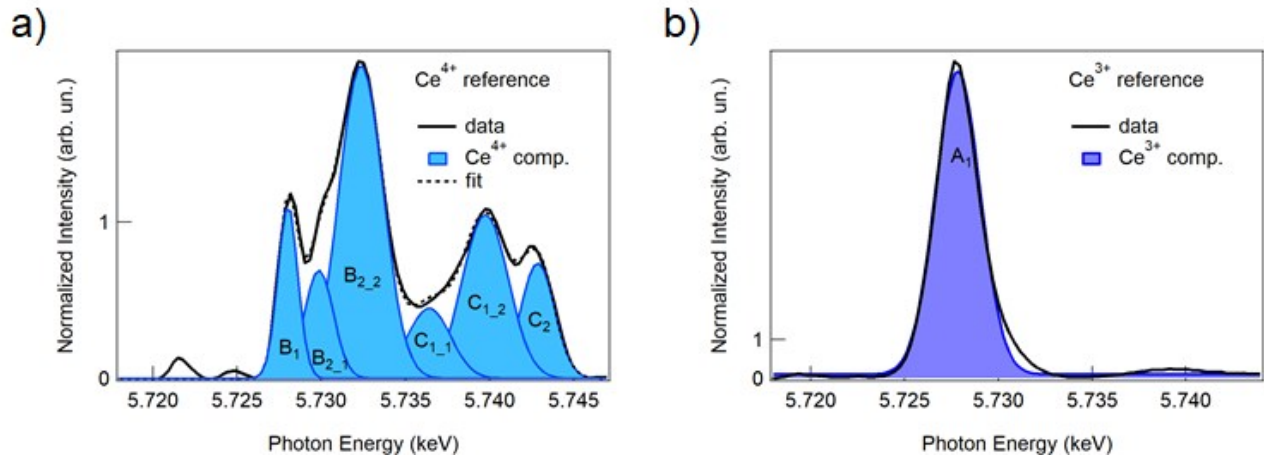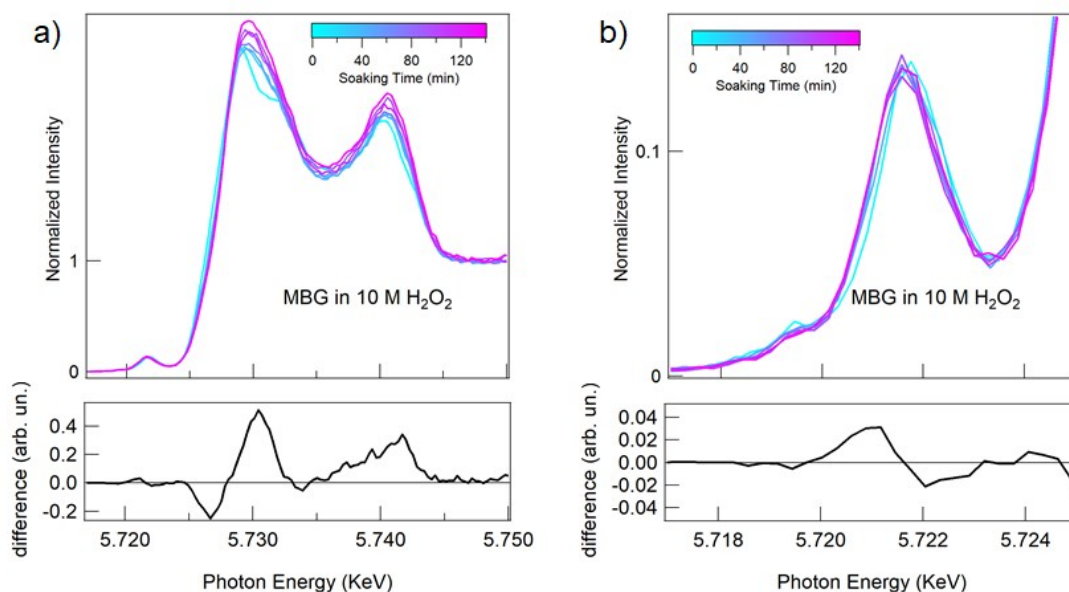
Figure S2: Ce L_3-edge HERFD-XANES spectra for the two reference samples for Ce^{4+} (a) and Ce^{3+} (b) (solid lines) after subtraction of the edge-jump modelled as an arctan function. The spectra were acquired on a CeO_2 sample and on a cerium nitrate hexahydrate $(Ce(NO_3)_3 \cdot 6H_2O)$ sample, respectively, in the form of powders pelleted with cellulose, with a cerium oxide concentration comparable to the one of glass samples. The individual Gaussian fitting components (solid blue) and the overall fits (dashed lines) are also shown. The A_1 peak in Ce^{3+} and the B_1 peak in Ce^{4+} are very close in energy, therefore only the A_1 component was used in the glass spectra fitting. The amplitude of the B_1 component was instead fixed to ratio $B_1/(B_2+C_1+C_2)$ in the Ce^{4+} reference, the amplitude of B_2, C_1 and C_2 being fitting parameters.
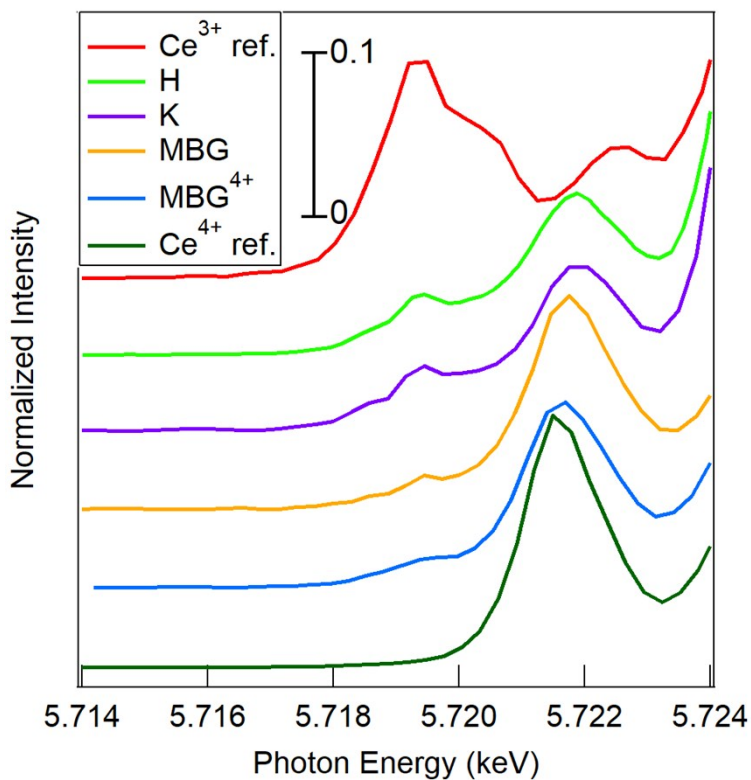
Figure S3: Ce L_3 pre-edge features of Ce^{3+} (red) and Ce^{4+} (dark green) reference samples and of the H (green), K (purple), MBG (orange), and MBG^{4+} (blue) glasses measured in pure water before the reaction. The pre-edge structures of the H and K samples exhibit a similar shape, with a dominant peak energetically close to the Ce^{4+} pre-edge peak (5.722 keV) and a further minor feature, close to the dominant peak of the Ce^{3+} reference spectrum (5.719 keV). In the MBG and MBG^{4+} samples the Ce^{3+} related peak has a progressively lower intensity compared to the H and K samples. The differences in the shape of the pre-edge features in the different samples are in qualitative agreement with the ones observed in the XANES region, thus supporting the simplified approach of considering the XANES of the glass samples merely as a superposition of Ce^{3+} and Ce^{4+} related components.
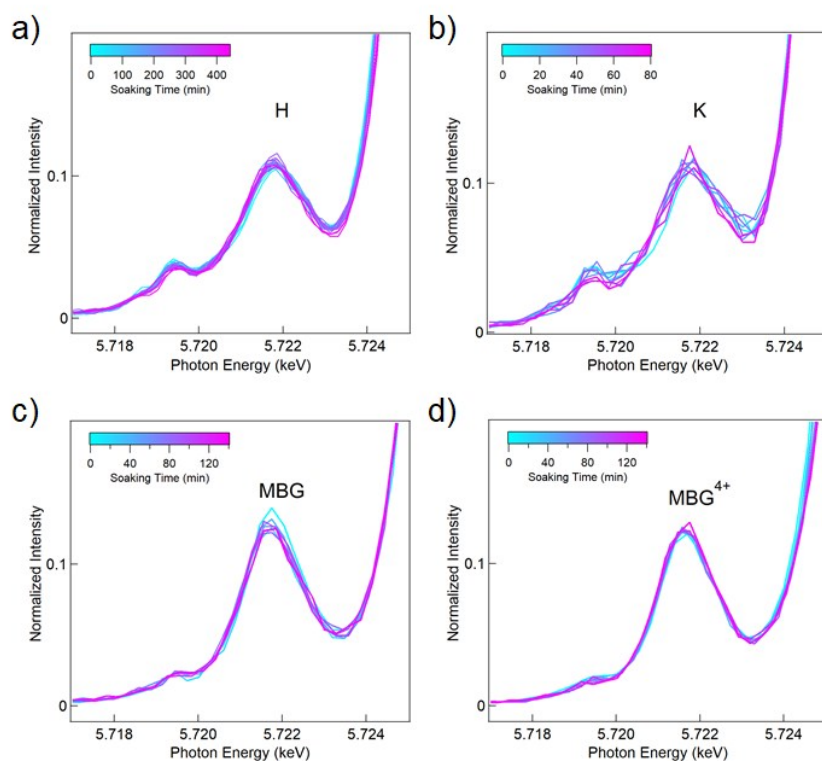
Figure S4: Evolution of the Ce L_3 HERDF-XANES spectra in the pre-edge region of H (a), K (b), MBG (c), and MBG^{4+} (d) glasses during the reaction with a 0.1 M H_2O_2 solution. The modifications induced in the pre-edge region by the reaction, although less evident than the ones observed in the edge region, are in agreement with a progressive oxidation of the samples, with the feature at 5.722 keV showing a mild increase and the one at 5.719 keV showing a mild decrease of intensity as the reaction proceeds.

Figure S5: Evolution of the Ce L_3-edge HERFD-XANES spectra of the MBG glass during the reaction with a 10 M H_2O_2 solution (top) and difference between the spectra after 140 min and before the reaction (bottom) for: a) the full XANES energy region; b) the pre-edge region. The spectral modifications are expectedly more significant than in the case of a 0.1 M solution. The difference spectrum in panel a shows a negative peak at 5.727 KeV, ascribed to shift of the edge jump to higher photon energies as the reaction proceeds, consistent with a mild oxidation. The two positive peaks correspond to increases in intensity at photon energies close to B_2 and C_1. The modifications of the pre-edge peak are limited to a very small shift to lower photon energies, consistent with a mild oxidation.

Goodness-of-fit parameters

The fitting program used for data fitting, Fitxk [6], uses the weighted sum of squared residuals x^2 as a function of $[y_i - f_i]$ for the fit. This is defined as:

$$\chi^2 = \sum_{i=1}^{N} \left[\frac{y_i - f_i}{\sigma_i} \right]^2$$

where y_i are the data points, f_i are the fitting points and σ_i are the standard deviations. The x^2 values of the fitting of the different samples are reported on table ST2. Table ST3 reports the R^2 values defined as:

$$R^2 = 1 - \frac{\sum_{i=1}^{N}(y_i - f_i)^2}{\sum_{i=1}^{N}(y_i - \bar{\bar{y}})^2}$$

where $\bar{\bar{y}}$ is the average of the data.

Table ST2: χ^2 values of the fittings of the different samples at different reaction times

reaction time (min) / sample	0	20	40	60	80	100	120	140
H	0.146284	0.159337	0.153525	0.155452	0.159839	0.138813	0.150275	0.163833
K	0.31115	0.288378	0.333766	0.262755	0.333889			
MBG	0.141338	0.104471	0.108194	0.097058	0.111457	0.094219	0.103882	0.098498
MBG^{4+}	0.035461	0.041338	0.055731	0.056533	0.068842	0.070865	0.076428	0.073068
MBG 10 M	0.141351	0.122776	0.142553	0.159438	0.193424	0.220339	0.21497	0.265112

Table ST3: R^2 values of the fittings of the different samples at different reaction times

reaction time (min) / sample	0	20	40	60	80	100	120	140
H	0.996951	0.996602	0.996679	0.996637	0.996463	0.996909	0.996668	0.996402
K	0.993327	0.993086	0.992524	0.993729	0.992486			
MBG	0.99645	0.997319	0.997267	0.9974	0.997031	0.997602	0.99728	0.997346
MBG^{4+}	0.999014	0.998892	0.998499	0.998537	0.998224	0.998177	0.998108	0.998188
MBG 10 M	0.999014	0.998892	0.998499	0.998537	0.998224	0.998177	0.998108	0.998188

References

1. S. Brunauer, P. H. Emmett and E. Teller, *J Am Chem Soc*, 1938, **60**, 309-319.
2. Patricia Balderas-Hernandez, Jorge G. Ibanez, Juan Jose Godinez-Ramirez and F. Almada-Calvo, *The Chemical Educator*, 2006, **11**, 267.
3. Jorge G. Ibanez, Margarita Hernandez-Esparza, Carmen Doria-Serrano, Arturo Fregoso-Infante and M. M. Singh, *Environmental Chemistry Microscale Laboratory Experiments*, Springer, New York, 2008.
4. T. Mahmood, M. T. Saddique, A. Naeem, P. Westerhoff, S. Mustafa and A. Alum, *Industrial & Engineering Chemistry Research*, 2011, **50**, 10017-10023.
5. V. Nicolini, E. Gambuzzi, G. Malavasi, L. Menabue, M. C. Menziani, G. Lusvardi, A. Pedone, F. Benedetti, P. Luches, S. D'Addato and S. Valeri, *J Phys Chem B*, 2015, **119**, 4009-4019.

6.   M. Wojdyr, *Journal of Applied Crystallography*, 2010, **43**, 1126-1128.